Photocytotoxic Pt(IV) complexes as prospective anticancer agents

Giovanni Canil[1]; Simona Braccini[1]; Tiziano Marzo[2]; Lorella Marchetti[1]; Alessandro Pratesi[3]; Tarita Biver[1, 2]; Tiziana Funaioli[1]; Federica Chiellini[1]; James D. Hoeschele[4]; Chiara Gabbiani[1 *]*

[1] Department of Chemistry and Industrial Chemistry (DCCI), University of Pisa, Via Moruzzi, 13, 56124 Pisa, Italy;

[2] Department of Pharmacy, University of Pisa, Via Bonanno Pisano 6, 56126, Pisa, Italy;

[3] Laboratory of Metals in Medicine (MetMed), Department of Chemistry "U. Schiff", University of Florence, Via della Lastruccia 3, 50019 Sesto Fiorentino, Italy;

[4] Department of Chemistry, Mark Jefferson Science Complex, Eastern Michigan University, Ypsilanti, Michigan, 48197, USA.

ABSTRACT

The oxidation of the Pt(II) compound **[PtCl(4'-phenyl-2,2':6',2"-terpyridine)][CF$_3$SO$_3$]** (**1**) with PhICl$_2$ and H$_2$O$_2$ is described. PhICl$_2$ produced the Pt(IV) complex with chlorides in the axial position, **[PtCl$_3$(4'-phenyl-2,2':6',2"-terpyridine)][CF$_3$SO$_3$]** (**2**). H$_2$O$_2$ oxidation and post-synthesis carboxylation with acetic anhydride produced **[Pt(OCOCH$_3$)$_2$(4'-phenyl-2,2':6',2"-terpyridine)Cl][CF$_3$SO$_3$]** (**3**), bearing acetates in the axial positions. **2** and **3** are stable in physiological-like conditions as well as in DMSO and undergo photoreduction to the Pt(II) complex **1** upon irradiation at 365 nm. The electrochemistry of the Pt(IV) complexes revealed an irreversible process that was attributed to the reduction Pt(IV) → Pt(II), confirming the greater stabilization given by the acetate axial groups, with respect to chlorides, toward reduction. The binding ability of **1** toward DNA was assessed with spectrophotometric titrations: most likely, **1** interacted via direct binding to the base pairs. The cytotoxic potency of **2** and **3** toward the human ovarian cancer cells A2780 either sensitive or resistant to cisplatin has been assessed and **3** was characterized by photocytotoxic properties. To gather insight in the mechanistic aspects of their pharmacological activity, bioinorganic studies have been carried out. The interaction with model proteins and single stranded DNA has been explored through high-resolution mass spectrometry and revealed that **2** and **3** behave as prodrugs, being able to bind to biological targets only when irradiated.

INTRODUCTION

In the last decades many attempts to overcome the recurrent problems of platinum-based chemotherapy have been made. Thousands of metal-based complexes, either Pt-based or bearing different metal centers have been synthesized and tested, but beyond cisplatin, only carboplatin, oxaliplatin and arsenic oxide (trisenox™) have been approved for the clinical use.[1-4] A suitable strategy to overcome the acute toxicity of the Pt(II) anticancer drugs relies on the use of Pt(IV) compounds, which are kinetically more inert. The lack of reactivity limits the unwanted side-reactions with biomolecules in the body, that are likely responsible for side effects of conventional platinum drugs.[5] The pharmacological action of Pt(IV) is believed to be exerted only after the reduction to the active Pt(II) species.[6] Since reduction is a crucial step, the reduction potential of the Pt(IV) prodrug is a feature of primary importance for a practical use. Compounds that are reduced very easily can give rise to severe side effects, while compounds that are very difficult to reduce can be excreted from the body without causing any therapeutic effect. In this view, it is possible to tune the reduction potential of the Pt(IV) compounds varying the coordination sphere of the metal centre. It has been found that the axial ligands are the major responsible for the stability of the complex: hydroxides impart the greater stability, while chlorides have a poor stabilization effect, and the acetates lie in between.[7]

The activation process may occur within the cells, due to their reducing environment, or it may happen as a consequence of an external stimulus, like the absorption of light. It is long known that light can cause the reduction from Pt(IV) to Pt(II),[8] but Bednarski and colleagues were the first group to exploit this feature with the purpose of chemotherapy in mind.[9] Their rationale consisted in the assumption that it was possible to induce the Pt(IV) reduction specifically at the tumor site, to selectively generate the Pt(II) species, which is pharmacologically-active. Therefore, they synthesized the compound *trans, cis*-[PtCl$_2$I$_2$(en)], which should release the iodide ligands after the photoreduction, to produce the *cis*-[PtCl$_2$(en)], the effective anticancer agent.[10] Despite the intriguing rationale, the molecule was not studied further because it was unstable in the presence of serum. Nevertheless, a major breakthrough in this field was reported by the group of Sadler and colleagues, which synthesized Pt(IV) compounds with azides as leaving ligands.[11] Among them, the one that exhibits the most favourable features is *trans, trans, trans*-[Pt(N$_3$)$_2$(OH)$_2$(py)$_2$], which is stable toward reduction and can be activated not only with UV, but also with blue and green light, even if its absorption maximum is around 295 nm.

In this frame, we designed a new class of unconventional monocationic Pt(IV) compounds, which bear the π conjugated ligand 4'-Phenyl-2,2':6',2"-terpyridine (phterpy), to shift the absorbance of the complexes in the visible range. The ligand should act as an antenna, promoting the reduction of the Pt(IV) complexes after absorption of light and may also impart the required stability necessary to obtain only one photoproduct, avoiding the formation of multiple species. The design of our molecules is different with

respect to the "classical" platinum anticancer drugs (general structure [PtX$_2$A$_2$], with X=anion and A=ammine) and therefore we expect different modes of action. To the best of our knowledge, only one example of a similar Pt(IV)-terpy complex is reported in literature,[12] but it has never been investigated as a photoactivated compound.

The benefits of an inert prodrug that is activated only at the site of interest after absorption of external light are priceless. Though, this task is not easy to accomplish: the Pt(IV) prodrug should be sufficiently stable, inert and soluble in the biological environment; it must be readily reduced after absorption of light and, finally, should display a good anticancer activity once reduced.

EXPERIMENTAL SECTION

General Considerations

All reagents and solvents were of reagent grade and used without further purification unless otherwise stated. ODN2 GGrich 10^{-3} M solution in MilliQ water, RNase A (type XII-A) and calf thymus DNA (CT-DNA, lyophilized sodium salt) were purchased from Aldrich. L-Glutahione, reduced (GSH) was purchased from AlfaAesar and had a purity of > 98%. Water was purified with ionic exchange resin and DMSO was of the highest grade available (Aldrich, 99.9%).

NMR measurements were recorded with a Varian Gemini 200BB spectrometer or a Bruker Avance II DRX400 instrument equipped with a BBFO broad-band probe. All spectra were run at room temperature. NMR chemical shifts (δ) are reported in parts per million (ppm) and referenced as described below. ^{1}H and ^{13}C{^{1}H} NMR spectra are referenced internally to residual solvent peaks, and chemical shifts are expressed relative to tetramethylsilane, Si(CH$_3$)$_4$. ^{195}Pt{^{1}H} NMR spectra are referenced externally using standards of K$_2$PtCl$_6$ in H$_2$O. Samples were prepared in DMSO-d$_6$ at room temperature. All samples (Pt(IV) compounds kept in the dark) showed no decomposition for at least one week under these conditions.

Carbon, hydrogen, and nitrogen analyses were performed on a Vario MICRO cube instrument (Elementar).

IR spectra of neat samples were recorded with a Perkin Elmer "Spectrum One" FT-IR spectrometer, with ATR technique.

Synthesis

Caution! Hydrogen peroxide must not come in contact with organic solvents that can form explosive peroxides. All synthesis and purifications were carried out under dim light conditions, avoiding contact with direct light.

4'-phenyl-2,2':6',2"-terpyridine (phterpy),[13] PhICl$_2$[14] and [PtCl$_2$(COD)] (COD = 1,5-cyclooctadiene)[15] were synthesized according to procedures previously reported in the literature and their purity was confirmed by NMR spectroscopic analysis and elemental analysis (see Supporting Information, SI, for characterization details).

[PtCl(phterpy)][CF$_3$SO$_3$] (1). This compound was synthesized using a modification of a previously reported procedure.[16] AgCF$_3$SO$_3$ (0.536 g, 2.09 mmol) was dissolved in a mixture of 12 mL of CH$_2$Cl$_2$ and 2 mL of CH$_3$CN and then dropped into a stirred solution of PtCl$_2$(COD) (0.707 g, 1.89 mmol) in 30 mL of CH$_2$Cl$_2$. After 30 minutes of stirring in the dark, AgCl was filtered off through a Celite pad. The resulting colorless solution was dropped into a stirred solution of phterpy (0.644 g, 2.08 mmol) in 35 mL of CH$_2$Cl$_2$. After the addition of a few drops, the color of the phterpy solution turned yellow, then an orange suspension resulted, which turned red after several minutes. The mixture was stirred for three days at room temperature and then filtered. The solid was washed with CH$_2$Cl$_2$ and diethyl ether and then dried *in vacuo*. Yield 1.204 g, 92%.

^{1}H NMR (DMSO-d_6, 400 MHz, 298 K): (Protons are labelled according to Scheme 1) δ 9.02 (s, 2H, H3'); 8.98 (m, $^3J_{HH}$ = 5.7 Hz, 2H, H6); 8.88 (m, $^3J_{HH}$ = 8.0 Hz 2H, H3); 8.57 (m, $^3J_{HH}$ = 8.0 Hz, $^3J_{HH}$ = 7.8 Hz, 2H, H4); 8.21 (m, 2H, Ha); 7.99 (m, $^3J_{HH}$ = 7.8 Hz, $^3J_{HH}$ = 5.7 Hz, 2H, H5); 7.70 ppm (m, 3H, Hb, c). ^{13}C NMR (DMSO-d_6, 100 MHz): δ 157.9, 154.1, 152.6 (quaternary carbons); 151.0 (C6); 142.5 (C4); 134.4 (quaternary carbon); 131.7 (Cc); 129.4 (Cb); 129.1 (C5); 127.9 (Ca); 126.1 (C3); 121.3 ppm (C3'). [195]Pt NMR (DMSO-d_6, 43 MHz): δ -2698 ppm. Anal. Calcd (%) for C$_{22}$H$_{15}$ClF$_3$N$_3$O$_3$PtS: C 38.35, H 2.19, N 6.10. Found: C 38.12, H 2.07, N 6.10.

[PtCl$_3$(phterpy)][CF$_3$SO$_3$] (2).

PhICl$_2$ (0.120 mmol) was added to a stirred solution of **1** (0.0688 g, 0.100 mmol) in DMF (4 mL). After stirring overnight in the dark, the volume was reduced (*ca.* 1 mL) until precipitation of a pale yellow solid begun. 50 mL of diethyl ether were added to complete the precipitation. The pale yellow solid was recovered by filtration, washed with diethyl ether and dried under vacuum. Yield 0.0696 g, 92%.

^{1}H NMR (DMSO-d_6, 400 MHz): (Protons are labelled according to Scheme 1) δ 9.48 (s, 2H, H3'); 9.25 (dd, $^3J_{PtH}$ = 25 Hz, $^3J_{HH}$ = 5.8 Hz, $^4J_{HH}$ = 1.2 Hz, 2H, H6); 9.24 (dd, $^3J_{HH}$ = 8.1 Hz, $^4J_{HH}$ = 1.3 Hz, 2H, H3); 8.80 (ddd, $^3J_{HH}$ = 8.1 Hz, $^3J_{HH}$ = 7.9 Hz, $^4J_{HH}$ = 1.2 Hz, 2H, H4); 8.30 (m, 2H, Ha); 8.25 (ddd, $^3J_{HH}$ = 7.9 Hz, $^3J_{HH}$ = 5.8 Hz, $^4J_{HH}$ = 1.3 Hz, 2H, H5); 7.77 ppm (m, 3H, Hb, c). ^{13}C NMR (DMSO-d_6, 100 MHz): δ 156.5 (quaternary carbon); 151.5 (C6); 151.0 (quaternary carbon); 145.1 (C4); 134.1 (quaternary carbon); 132.5 (Cc); 131.6 (C5); 129.6 (Cb); 129.3 (C3); 128.8 (Ca); 125.6 ppm (C3'). [195]Pt NMR (DMSO-d_6, 43 MHz): δ -562 ppm. Anal. Calcd (%) for C$_{22}$H$_{15}$Cl$_3$F$_3$N$_3$O$_3$PtS: C 34.77, H 1.99, N 5.53. Found: C 34.85, H 1.84, N 5.65.

[Pt(OCOCH$_3$)$_2$(phterpy)][CF$_3$SO$_3$] (3).

To a suspension of **1** (0.0563 g, 0.0817 mmol) in 5 mL of glacial acetic acid, 2.0 mL of 30% H_2O_2 (19.4 mmol) were added. After 64 hours of stirring in the dark at room temperature a pale yellow solution resulted. All the volatiles were evaporated under reduced pressure and then 10 mL of deionized water were added. The pale yellow suspension formed was stirring for 20 minutes, then the solvent was evaporated and the residue dried in vacuo. 5 mL of acetic anhydride (51.8 mmol) were added to the solid, yielding a solution at first, then a white thin precipitate started to form and, after 30 hours of stirring in the dark, 80 mL of diethyl ether were added to complete precipitation. The solid was collected by filtration, thoroughly washed with diethyl ether and dried under reduced pressure. Yield 0.0620 g, 92%.

^{1}H NMR (DMSO-d_6, 400 MHz): (Protons are labelled according to Scheme 1) δ 9.37 (s, 2H, H3'); 9.29 (dd, $^3J_{HH}$ = 5.8 Hz, $^4J_{HH}$ = 1.2 Hz, 2H, H6); 9.11 (dd, $^3J_{HH}$ = 8.0 Hz, $^4J_{HH}$ = 1.2 Hz, 2H, H3); 8.71 (ddd, $^3J_{HH}$ = 8.0 Hz, $^3J_{HH}$ = 7.9 Hz, $^4J_{HH}$ = 1.2 Hz, 2H, H4); 8.31 (m , 2H, Ha); 8.16 (ddd, $^3J_{HH}$ = 7.9 Hz, $^3J_{HH}$ = 5.8 Hz, $^4J_{HH}$ = 1.2 Hz, 2H, H5); 7.76 (m, 3H, Hb, c); 1.60 ppm (s, 6H, H7). ^{13}C NMR (DMSO-d_6, 100 MHz): δ 174.6 (acetate C=O); 157.9, 156.2 and 153.0 (quaternary carbons); 152.0 (C6); 144.6 (C4); 134.0 (quaternary carbon); 132.4 (Cc); 130.2 (C5); 129.6 (Cb); 128.6 (Ca); 127.5 (C3); 123.4 (C3'); 21.4 ppm (CH$_3$). [195]Pt NMR (DMSO-d_6, 43 MHz): δ 712 ppm. Anal. Calcd (%) for $C_{26}H_{23}ClF_3N_3O_8PtS$ (**3**·H_2O): C 37.85, H 2.81, N 5.09, S 3.89. Found C 38.10, H 2.93, N 5.00, S 3.75. ESI-MS: 657.04 Da (molecular ion, positive mode). IR: 1650 (br) cm^{-1}.

LogP determination

The octanol–water partition coefficients of the complexes were determined by modification of the reported shake-flask method.[17] Briefly, equal volumes of milli-Q water and n-octanol were shaken together for 72 h to allow saturation of the two phases. Next, solutions of the complexes were prepared in the saturated water phase (5×10^{-4} M) and an equal volume of octanol was added. Biphasic solutions were mixed for ten minutes and then centrifuged for five minutes at 6000 rpm to allow separation. The concentration of both phases was determined by UV-Vis spectroscopy. The reported *logP* value is defined as $\log[\text{complex}]_{oct}/[\text{complex}]_{wat}$ and is the mean of three determinations.

UV-Vis studies

UV-Visible electronic spectra were recorded with a Perkin Elmer λ650 or a Cary 60 UV-Vis spectrophotometer in 1.0 cm path length quartz cuvettes at room temperature, using DMSO or an aqueous buffered solution (sodium cacodylate = 0.1 M, [Cl$^-$] = 7×10^{-3} M, pH=7.3, DMSO content less than 2%) as solvents. The pH-Meter used was a Ω Metrohm 713.

Stability. The stability of the complexes in aqueous buffer was assessed evaluating their absorption spectrum for 24 hours, in the range between 230 and 600 nm, at 25 °C. For **2** and **3** it was mandatory to

record the spectra keeping the solutions in the dark, because they are not stable when in contact with light. Therefore, a mother solution was prepared at time 0 and aliquots of this solution were analyzed repeatedly. We discarded the solution in the cuvette after the measurement, in order to be sure that the light of the spectrophotometer was not having an effect on the stability.

Irradiation. Irradiation was performed with a UV lamp Spectroline™ model ENF-260C/F (230 volts, 50 Hz, 0.17 A), Spectronics corporation Westbury, New York, USA, operating at 365 nm. The power of the lamp was measured with a detector at a distance of 12 cm and was found to be 5.5 mW×cm^{-2}. Solutions of **2** and **3** were irradiated at 365 nm and their electronic spectra recorded at different time intervals, until the last absorption profile did not change appreciably with respect to the precedent one.

Time constants evaluation. The variation of A as a function of irradiation time resulted in an exponential decay, typical of a first order kinetic law [1997 logan]. We plotted the logarithm of A against the irradiation time, obtaining a first order function that has the slope -1/τ. The procedure was repeated for 4 different wavelengths, at which the variation was maximum, to have the mean value.

Electrochemistry

Electrochemical measurements were recorded on a PalmSens4 instrument interfaced to a computer employing PSTrace5 electrochemical software, and were performed in DMSO solutions containing [N^{n}Bu$_4$][CF$_3$SO$_3$] (0.1 M) as the supporting electrolyte at room temperature. Electrochemical grade [N^{n}Bu$_4$][CF$_3$SO$_3$] (Fluka) and ferrocene (Cp$_2$Fe, Fluka) were used without further purification.

Cyclic voltammetry (CV). CV was performed in a three-electrode cell, having a Teflon encapsulated carbon-glassy working electrode, a platinum-gauze counter electrode and a platinum quasi reference electrode. Prior to measurements, the glassy-carbon working electrode was polished according to the following procedure: manual rubbing with 0.3 μm Al$_2$O$_3$ slurry in water (eDAQ) for 2 min, then sonication in ultrapure water for 10 min, manual rubbing with 0.05 μm Al$_2$O$_3$ slurry in water (eDAQ) for 2 min, then sonication in ultrapure water for 10 min. The solution of supporting electrolyte was introduced into the cell, and deaerated by bubbling Ar for several minutes. The potential of the working electrode was cycled several times between the cathodic and anodic limits to determine the solvent window. The analyte was then introduced in the cell with a concentration of $< 1 \times 10^{-3}$ M, Ar was bubbled again and the voltammograms were recorded (0.1 V/s); then a small amount of Cp$_2$Fe was added and a further voltammogram was recorded. Potentials were determined by placing the Cp$_2$Fe$^+$/Cp$_2$Fe couple at 0.0 V.[20] Under the present experimental conditions, the one-electron oxidation of Cp$_2$Fe occurs at E° = +0.50 V *vs* Ag/AgCl$_{(aq)}$. In the case of Pt(IV) compounds, the cell was covered with aluminum foil to avoid direct light.

Hydrodynamic voltammetry (linear sweep voltammetry, LSV). LSV with renewal of the diffusion layer made use of a rotating disk electrode Metrohm 628-10, consisting of a glassy carbon with an insulating teflon surrounding.

Electrolysis. Controlled potential Coulometry was performed in an H-shaped cell with anodic and cathodic compartments separated by a sintered-glass disk. The working macro-electrode was a glassy carbon stick; the counter electrode was a platinum spiral and the reference electrode was Ag|AgCl|KCl (sat.), mounted with a salt bridge containing the electrolyte\NBu$_4$PF$_6$ in DMSO and separated from the solution by a Vycor frit. 10 ml of a 6.3×10^{-4} M solution of compound **2** was electrolyzed at -0.5 V for 3700 s; the total charge flowed in the electrolytic cell was 447 mC, corresponding to 4.6 µeq of electrons, that means 2.3 µmol of Pt(II) formed from the two-electrons reduction of Pt(IV) (initial amount of Pt = 6.3 µmol), equivalent to 37 % of conversion. An aliquot of both the initial and the electrolyzed solution was diluted with DMSO to a Pt final concentration of 4×10^{-5} M and the absorbance at 405 nm was recorded (Figure S21 SI). The Pt(II) concentration was assessed by interpolation of the height of the peak at 405 nm with a calibration curve (Figures S22-S23 SI), giving an Pt(II) concentration of 1.48 10^{-5} M, that was the 37% of the initial Pt(IV).

Cellular Studies

Human ovarian carcinoma cisplatin-sensitive A2780 (ECACC 93112519) and human ovarian carcinoma cisplatin-resistant A2780cis cell lines (ECACC 93112517) were purchased from European Collection of Authenticated Cell Cultures (ECACC). Cell proliferation reagent WST-1, cisplatin, RPMI 1640 medium, Dulbecco's Phosphate Buffer Saline (DPBS), fetal bovine serum (FBS), L-glutamine and penicillin:streptomycin solution were purchased from Sigma-Aldrich (Milan, Italy). Plasmocin™ was purchased from InvivoGen (San Diego, Usa). Earle's Balanced Salts solution (EBSS) was prepared by dissolving 0.2 g of CaCl$_2$, 0.1 g of MgSO$_4$, 0.4 g of KCl, 6.8 g of NaCl, 0.14 g of NaH$_2$PO$_4$◇H$_2$O, 1 g of D-glucose and 2.2 g of NaHCO$_3$ in 1 L of distilled water. The final pH was adjusted to 7.4 and the solution was sterile-filtered (0.22 µm) before use.

Cell culture. A2780 and A2780cis cell lines were propagated as indicated by the supplier using RPMI 1640 medium and supplemented with 2×10^{-3} M of L-glutamine, 1 % of penicillin/anstreptomycin solution (10,000 U/ml:10 mg/ml), 10% of FBS and antimycotic and were maintained under standard tissue culture conditions of 37 °C and 5% atmosphere of CO$_2$. The acquired resistance of A2780cis cells was maintained by supplementation of media with 1 µM of cisplatin every second passage.[22]

Cell viability assay. A2780 and A2780cis cells were seeded into 96-well culture plates at a concentration of 3×10^3 and 6×10^3 cells per well, respectively. Stock solutions of the selected compounds were prepared in DMSO at a concentration of 10 mM and then serially diluted in supplemented RPMI to achieve the

final desired concentrations. After overnight incubation, the cells were treated with different concentrations (0-100 µM) of the selected compounds for 72 hours. Then the cell viability was investigated by mean of WST-1 tetrazolium salt reagent. Briefly, cells were incubated for 4 hours with WST-1 reagent diluted 1:10, at 37 °C and 5% CO_2. Measurements of formazan dye absorbance were carried out with a microplate reader (Biorad, Milan, Italy) at 450 nm, using 655 nm as reference wavelength.

Phototoxicity assessment. A2780 and A2780cis cells were seeded into 96-well culture plates at a concentration of 1×10^4 and 1.5×10^4 cells per well, respectively, and left to adhere overnight. Stock solutions of the selected compounds were prepared in DMSO at a concentration of 10 mM and then serially diluted in EBSS to achieve the final desired concentrations. After washing the cells with DPBS, test compounds in EBSS were added (final concentration 0-50 µM) and incubated for 1 hour at 37 °C and 5% atmosphere of CO_2. Subsequently the cells were irradiated with UV light (λ=365 nm) for 6 minutes (delivering a light dose of 2 J$\times$cm^{-2}). Cells incubated with same amounts of DMSO in EBSS were used as control. Moreover, experiments were also performed adopting the above reported conditions but without irradiation. Following irradiation, the salt solution was removed, the cells were thoroughly washed and then returned to the incubator in complete growth medium. Phototoxicity was determined 24 hours later (recovery time) using WST-1 tetrazolium salt reagent. This procedure was similar to the one reported by Mackay *et al.*[23]

Pt uptake measurement. A2780 cells were seeded at a concentration of 1×10^6 and were allowed to proliferate for 24 hours before being incubated in complete medium containing 50 µM of the selected compounds, for 1h. At the end of the uptake period, the cells were quickly washed three times with DPBS, collected, counted (2.5×10^6 cells treated with **3** and 2.6×10^6 cells treated with cisplatin) and gently spun down (400 g for 5 min) and processed for ICP-AES analysis as described in the ICP analysis section.

Statistical analysis. All *in vitro* experiments were conducted in triplicate. Concentration effect curves were generated by nonlinear regression curve (GraphPad Prism) and the data are expressed as mean ± SD.

ICP analysis

The determination of metals concentration in the cell was performed as previously reported (Fabbrini et al ChemMedChem 2019 2019, 14, 182 – 188) by a Varian 720-ES inductively coupled plasma atomic emission spectrometer (ICP-AES) equipped with a CETAC U5000 AT+ ultrasonic nebulizer, in order to increase the method sensitivity. Before analysis, fixed volumes of samples were moved in vials and digested in a thermo-reactor at 80 °C for 3 h with 1 mL of

aqua regia (HCl supra-pure grade and HNO_3 supra-pure grade in 3:1 ratio) and 5 mL of ultrapure water (≤18 MΩ). Samples were spiked with 1 ppm of Ge used as an internal standard and analyzed. Calibration standards were prepared by gravimetric serial dilution from a commercial standard solution of Pt at 1000 mg×L^{-1}. The wavelength used for Pt was 214.424 nm, whereas for Ge the line at 209.426 nm was used. The operating conditions were optimized to obtain maximum signal intensity, and between each sample, a rinse solution of HCl supra-pure grade and HNO_3 supra-pure grade at a 3:1 ratio was used to avoid any "memory effect". The values of Pt were normalized to cells number.

ESI-MS Experiments: interaction with model targets

The ESI-MS study of the interactions with target biomolecules was performed in accordance with a well-established protocol[21] using an AB SCIEX TripleTOF 5600+ high-resolution mass spectrometer.

An aliquot of a stock solution of platinum complex in DMSO (usually $4×10^{-3}$ M, freshly prepared) was mixed with an aliquot of the target biomolecule dissolved in water (MilliQ) and diluted to a final concentration of 10^{-4} M for both species, with a final percentage of DMSO = 2.5%. All the operations and the incubation were done at room temperature. **1** was incubated at ambient light for 72 h. **2** and **3** were incubated in duplicate: one sample was kept in the dark throughout all the 72 hours incubation, while the other was initially irradiated for 5 minutes at 365 nm, then incubated for 72 hours in the dark. For the ESI-MS analysis, aliquots were sampled and diluted with LC-MS water to a final concentration of the species of 10^{-6} M. Respective ESI mass spectra were acquired through direct infusion at 7 μL×min^{-1} flow rate in the mass spectrometer. In the case of RNase A 0.1% of formic acid was added to the final sample solutions and the spectra were recorded in positive polarity. In case of ODN, 1% of triethylamine was added to the final sample solutions and the spectra were recorded in negative polarity. The ESI source parameters optimized in the case of RNaseA were: Ionspray Voltage Floating 5500 V, Ion source Gas 1 (GS1) 40; Ion source Gas 2 (GS2) 0; Curtain Gas (CUR) 30, Declustering Potential (DP) 200 V, Collision Energy (CE) 10 V. In the case of ODN: Ionspray Voltage Floating -4500 V, Temperature 400 °C, Ion source Gas 1 (GS1) 40; Ion source Gas 2 (GS2) 30; Curtain Gas (CUR) 25, Declustering Potential (DP) -30 V, Collision Energy (CE) -10 V. For the acquisition, Analyst TF software 1.7.1 (Sciex) was used and the deconvoluted spectra were obtained by using the Bio Tool Kit micro-application v.2.2 embedded in PeakView™ software v.2.2 (Sciex).

The ESI mass spectrum of **3** was obtained with an Acquity QDA mass detector interfaced with Acquity UPLC (Waters). The analysis was done with an ESI probe by flow injection in CH_3CN/H_2O (1:1) at a flow rate of 200 μL×min^{-1}. 10 μL were injected, the ESI capillary voltages were 1.5 (positive) and 0.8

(negative); the cone voltage was 15 V and the mass range observed was 100-1000 Da.

Interaction with CT-DNA

1 was dissolved in DMSO and then diluted (5×10^{-5} M) in the buffered solution. The CT-DNA (DNA hereafter) stock solution in MilliQ water was prepared according to procedures described in the literature.[18] The concentration of the DNA stock solution was precisely determined recording a UV-Vis spectrum ([NaCl] = 0.1 M; [NaCac] = 2.5×10^{-3} M, pH 7.0, λ = 260 nm, ε = 13200 $M^{-1}\times cm^{-1}$)[19] in triplicate, and the DNA concentration is expressed in base pairs. The interaction studies with DNA were evaluated with UV-Vis spectroscopy by titrating the platinum compound in aqueous sodium cacodylate with a solution of DNA with a precise concentration. Operatively, small amounts of DNA were added both in the cell containing the platinum compound and in the cell containing the reference, so that the absorbance due to the DNA would be corrected by this differential procedure. We performed the experiment at three different temperatures (18.6 °C, 25.0 °C and 36.5 °C). Despite the efforts to correct the signals from the DNA contribution, these data suffer of higher errors in the UV range due to the high DNA absorbance (maximum DNA concentration 2.6×10^{-4} M). However, a robust data analysis could be performed with the software HypSpec2014 (Hyperquad) where all the wavelengths from 300 to 600 nm (a region far from the DNA absorption) were analyzed and, through an iterative process, a reasonable equilibrium constant for the formation of the various species was output. Specifically, the species we are dealing with are free platinum complex **1**, the adduct formed between **1** and DNA in a 1:1 stoichiometry (**1P**) and the adduct (**1₂P**) which accounts for all the stoichiometries different from 1:1 related to metal complex excess conditions and with its crowding on the DNA surface). Note that the equilibrium constant for **1₂P** formation will thus be an apparent constant. Therefore, the quantitative analysis of the binding constants values was done for the formation of the **1P** monoadduct only.

RESULTS AND DISCUSSION

Preparation of complexes

The platinum (II) complex **1** was prepared by coordination of the ligand phterpy to the organometallic precursor [PtCl₂(COD)] with a modification of the literature procedure,[16] allowing a higher yield and a lower reaction temperature (25 °C). The synthesis of [PtCl₃(phterpy)][CF₃SO₃] (**2**) and of [Pt(OCOCH₃)₂Cl(phterpy)][CF₃SO₃] (**3**) were accomplished under dim light conditions in one or two steps, starting from **1** and the appropriate oxidant, as depicted in Scheme 1.

2 was obtained as a very pale yellow powder by reacting (for a few hours) a DMF solution of **1** with a slight excess of PhICl₂.

3 was prepared in two steps as depicted in Scheme 1, starting from a slurry of **1** in neat acetic acid with a large excess of H_2O_2. All the Pt(II) was considered oxidized when no solid was left in the reaction mixture (less than 12 hours). Removal of the volatiles (care was used in order to thoroughly remove H_2O_2) led to a mixture of products (Figure S1 SI), of which [Pt(OCOCH$_3$)Cl(OH)(phterpy)][CF$_3$SO$_3$] was the major component. Finally, treatment of the crude mixture intermediate with excess acetic anhydride (used as solvent) led to the desired bis-acetato **3**, obtained as a white precipitate.
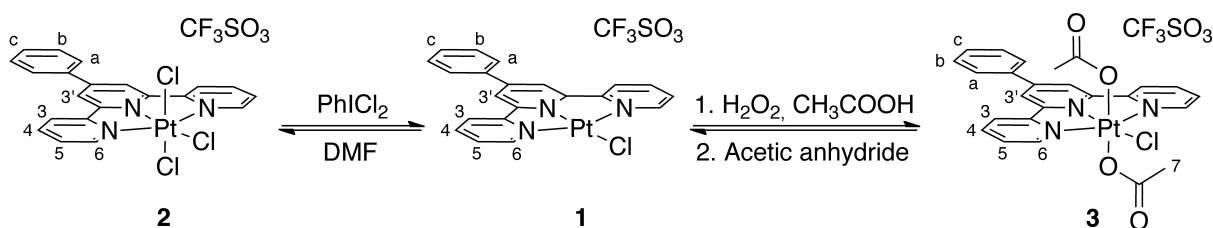
Scheme 1. Oxidation of **1** to produce **2** and **3** and selected spectral features.

We also tried to obtain the mono-acetato Pt(IV), [Pt(OCOCH$_3$)Cl(OH)(phterpy)][CF$_3$SO$_3$], as a pure species, varying the reaction time. However, for shorter reaction times the mixture was contaminated with another Pt(IV) compound (possibly the one with two hydroxides in the axial position, Figure S1 SI), while for longer reaction times the product with two acetates in the axial position (**3**), begun to form. The mono-acetato mono-hydroxo product, [Pt(OCOCH$_3$)Cl(OH)(phterpy)][CF$_3$SO$_3$], forms according to the oxidation mechanism of H_2O_2 in water, as proposed by Dunham *et al*:[24] the OH ligand coordinated to Pt(IV) derived from the oxidant and the second ligand (acetate) was taken from the solvent. Then, for longer reaction times, the OH coordinated to Pt(IV) could be protonated by acetic acid present as solvent, leading to loss of an aqua molecule and replacement by the acetate ligand. This replacement of the hydroxide by the acetate is slow due to the kinetic inertness of the Pt(IV) metal center and took several days for the product **3** to form spontaneously. On the other hand, for the rapid synthesis of **3**, we exploited the nucleophilicity of the OH ligand to operate an intermolecular carboxylation,[1] which was completed in a few hours.

The oxidation of **1** was confirmed by prominent changes in the NMR spectra. The resonances of the ^{195}Pt nuclei of **2** and **3** were found at -562 ppm, and 712 ppm, respectively, largely downfield shifted with respect to **1** (-2698 ppm). Also the ^{1}H nucleus experiences a downfield shift going from Pt(II) to Pt(IV): this is a consequence of the increased electronegativity of the metal center in the +4 oxidation state[25] and can be used as a quick detection of successful oxidation for our system. The ^{1}H NMR resonances of the Pt(II) precursor **1** are concentration dependent, as reported previously by Arena *et al*.[26] (Figure S2 SI). On the other hand, **2** and **3** are not concentration dependent (Figure S3 SI), indicating that the octahedral

arrangement of the Pt(IV) avoids the formation of π stacking interaction, thus hampering the formation of aggregates, as reported for systems similar to **1**.[27]

The IR carbonyl stretching at 1650 cm^{-1} is a confirmation of the coordination of the acetate ligand in compound **3** (free acetic acid has an absorption at 1715 cm^{-1}). Moreover, since in the ^{1}H NMR spectrum of **3** only one signal for the methyl group of the acetate was found, then only the *trans* isomer was formed.

Solution chemistry and *logP* evaluation

Given the poor aqueous solubility of the complexes, DMSO was used as preferred solvent. Since it is known that Pt(II) complexes like cisplatin exchange their chlorides in a DMSO solution, leading to inactivation of the drug[28], we had to test the stability of the Pt(II) species **1** in this coordinating solvent. ^{195}Pt NMR spectroscopy (Paragraph S2, SI) revealed that **1** could not dissociate its chloride in DMSO without the presence of a silver salt that facilitates the abstraction, precipitating as AgCl. Moreover, a cyclic voltammetry experiment confirmed the lack of chloride dissociation, showing no oxidation waves for the process Cl$^-$ → 1/2Cl$_2$ (Figure S4 SI) in DMSO.

DMSO stock solutions of **1**, **2** and **3** could be easily diluted in water or in sodium cacodylate buffer (NaAsO$_2$(CH$_3$)$_2$), where the interaction studies with DNA and target biomolecules were performed, in physiological-like conditions (DMSO content was less than 2%). The chemical stability was studied both in aqueous buffer, with the UV-Vis spectrophotometer, and in DMSO-d$_6$, with ^{1}H and ^{195}Pt NMR spectroscopy. The compounds were stable for at least 24 hours, as displayed in Figures S5÷S10 in SI.

Furthermore, since the lipophilicity of a complex is an important parameter involved in the cellular uptake, the partition coefficient *logP* was quantitated (Table S1 SI). The results obtained indicated a similar and small hydrophilicity for **1** and **2**, while **3** is one order of magnitude more soluble in water because of the presence of acetates. In fact, acetates are known to improve the water solubility of platinum compounds and are often used for this purpose.[29] Indeed, the intermediate complex in the synthesis of **3** (major component [Pt(OCOCH$_3$)Cl(OH)(phterpy)][CF$_3$SO$_3$]) was soluble in acetic anhydride but, as soon as the second acetate ligand was present in the coordination sphere, it precipitated out of the reaction mixture.

Irradiation studies

The photoreactions of **2** and **3** with 365 nm light were studied with UV-Vis spectroscopy. A DMSO solution of **3** was exposed to UV light directly in the cuvette and the spectra were recorded at increasing time intervals, Figure 1 A. The new band at 405 nm grew up and reached a plateau after 15 minutes of irradiation. At this time the photoreaction was almost complete and a profile similar to **1**, highlighted in

red in the Figure, was obtained. The presence of two well defined isosbestic points indicated a simple equilibrium in solution, attributable to the conversion of the Pt(IV) species into a reduced Pt(II) compound as the irradiation was going on. Figure 1 B shows the irradiation of **3** in aqueous sodium cacodylate. Now the isosbestic points are not perfect as the ones in DMSO solvent, a feature that could be interpreted considering multiple equilibria. The aquation reaction that follows the photoreduction of the Pt(IV) species might be the reason for this behaviour. The band at 390 nm, which we attributed to a Pt(II) species (possibly compound **1**), grows for subsequent irradiations until a total of 35 minutes of irradiation, when it reaches a plateau.
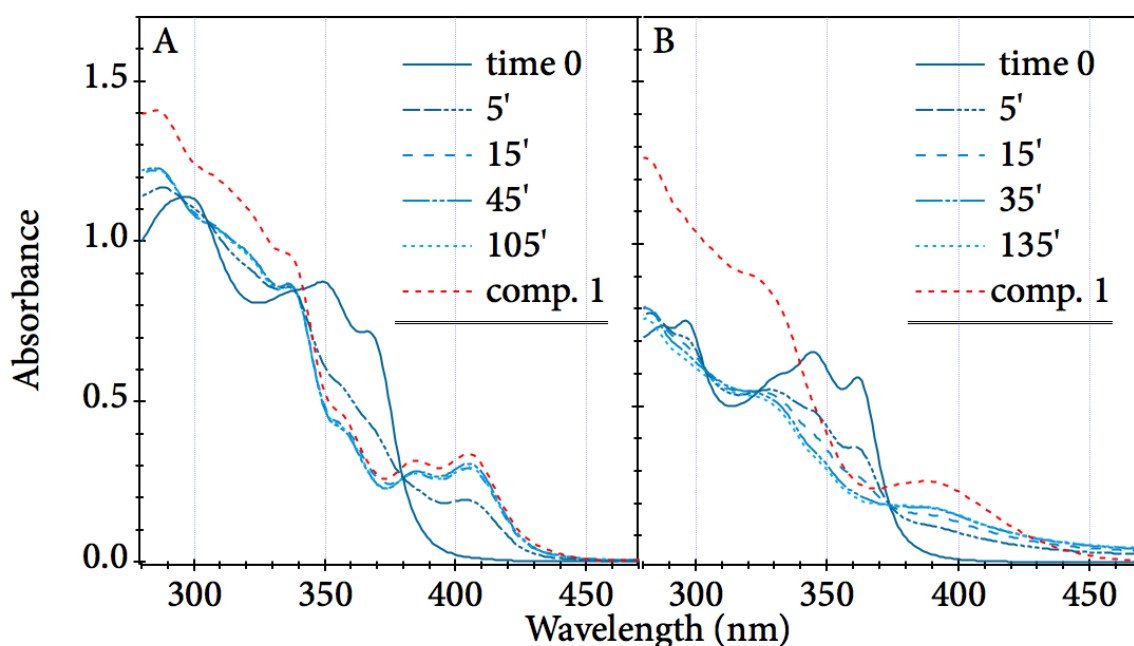

Figure 1. Irradiation of compound **3** in DMSO (A) and in aqueous buffer (B) with UV light at 365 nm; the irradiation time is given in the legend. In A, **3** (4.9×10^{-5} M) in DMSO is confronted with compound **1** (4.9×10^{-5} M) in the same solvent. In B, **3** (5×10^{-5} M) in sodium cacodylate 0.09 M solution ([Cl]$^-$ = 4×10^{-3} M, pH = 7.4, DMSO content 2%) is confronted with compound **1** (4.9×10^{-5} M) in the same solvent.

2 was studied in the same way as **3** (Figures S11-S12 in SI), *i.e.* in DMSO and in aqueous sodium cacodylate. Again, the photoreduction Pt(IV) → Pt(II) was over in more or less 15 minutes in DMSO, but was not over in the aqueous buffer even after more than 1 hour. We could compare the rate of the photoreductions of **2** and **3** in the various solvents once we found the values of the time constants, which are reported in Table S2 (SI). Compound **3** is reduced faster than **2** in both solvents, DMSO and aqueous buffer, at the wavelength used for irradiation (365 nm).

Our next evaluation pointed at determining what were the species present at the end of the photoreduction, *i.e.* their qualitative nature. In order to do so, we superimposed the absorption profiles of the irradiated **3** and **2** in DMSO at the end of the irradiation. It turned out that the absorption profiles were very similar between each other and with respect to **1** in the same solvent (Figure S13 SI). This suggests us that the irradiation leads to the Pt(II) precursor **1**, with dissociation of the axial ligands (chlorides for **2** and acetates for **3**) in DMSO solvent. This hypothesis was proved for **3**, which was dissolved in DMSO-d_6 and irradiated directly in the NMR tube, Figure 2. The irradiation proceeded for more than 4 hours (total light dose 92 J×cm^{-2}), until all the Pt(IV) was consumed and the Pt(II), which resonates at lower ppm, formed. Also, in the aliphatic region of the spectrum, we see that the bound acetate (methyl at 1.60 ppm) disappeared at the end of the irradiation, while the free acetate in solution (methyl at 1.91 ppm), grew up.
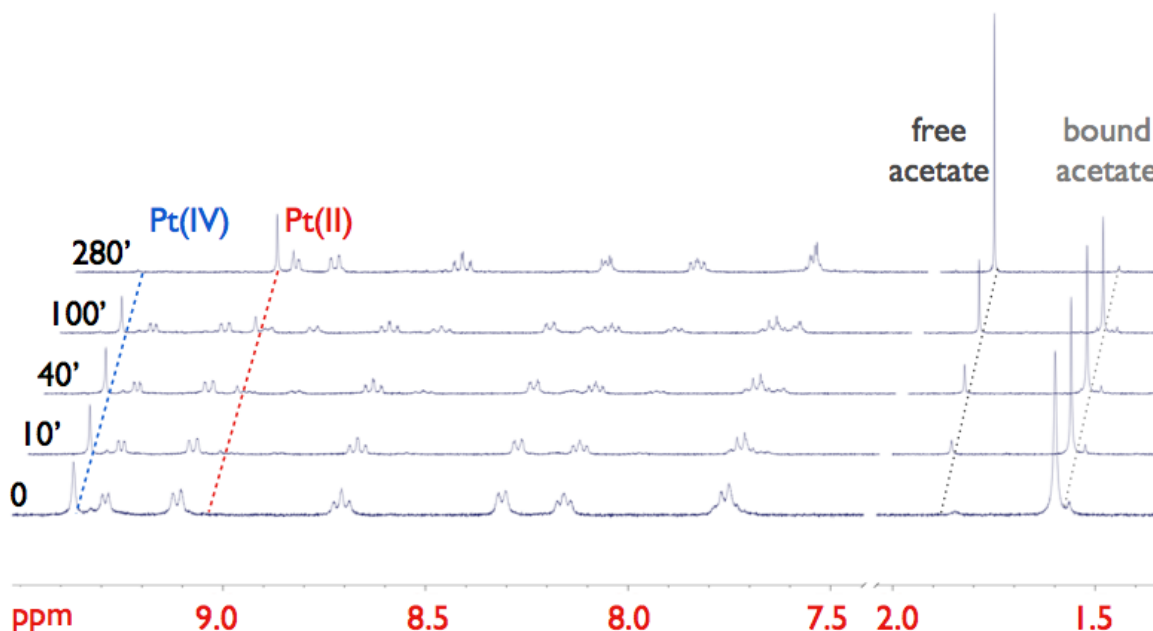

Figure 2. Irradiation of **3** (concentration 1.7×10^{-3} M) in DMSO-d_6 directly in the NMR tube. The total irradiation time is highlighted at the left of each spectrum.

Electrochemistry

After proving that **2** and **3** could be reduced to a Pt(II) species in a photoreaction with UVA light, we evaluated their reduction potential. In fact, in order to have a usable Pt(IV) prodrug, we need it to be stable in the reducing cellular environment and the ease of reduction is easily quantifiable with the electrochemical methods reported in this section. The cyclic voltammetries (CVs) of **1**, **2** and **3** are displayed in Figure 3 and the formal electrode potentials are compiled in Table 1.
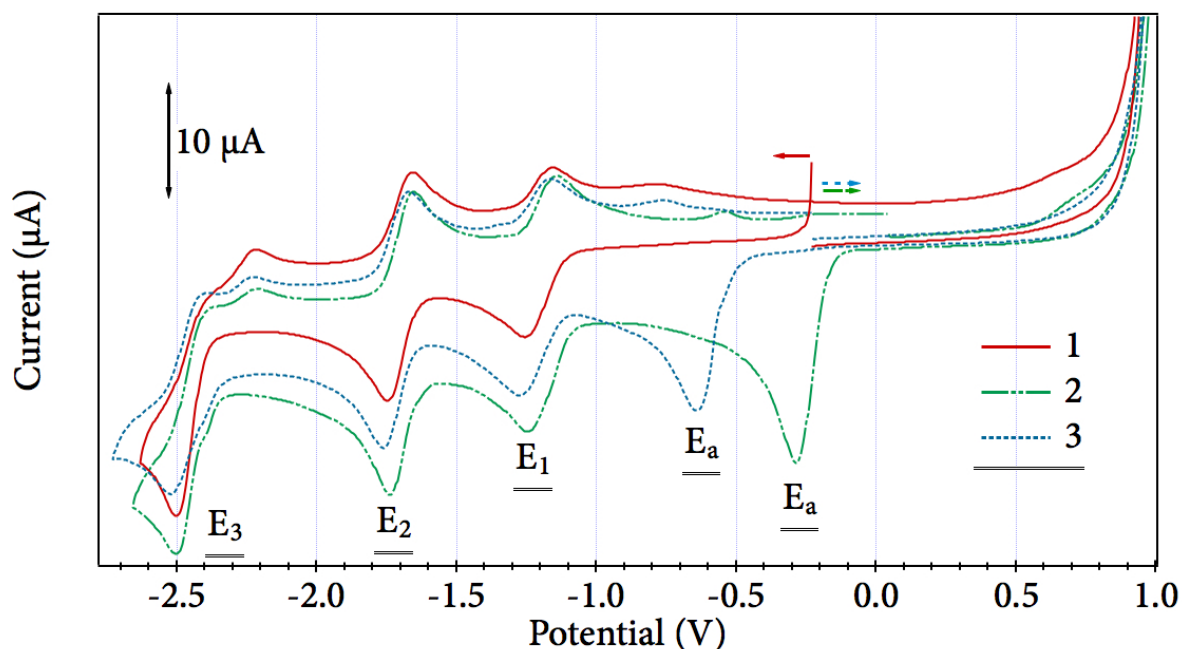
Figure 3. The CVs of the compounds **1**, **2** and **3** (1 mM) in DMSO with 0.1 M [N^{n}Bu$_4$][CF$_3$SO$_3$]. The direction of the arrows indicates the direction of the scan.

Table 1. Formal electrode potentials (V *vs* FeCp$_2$) and peak-to-peak separations (ΔE_p in mV) in 0.1 M [N^{n}Bu$_4$][CF$_3$SO$_3$]/DMSO solution for the cited redox changes.

Compound	E_a	$E°'_1$	$\Delta E_p(1)$ [a]	$E°'_2$	$\Delta E_p(2)$ [a]	E_3 [b]
phterpy		-2.36	95			
1		-1.21	99	-1.70	87	-2.50
2	-0.29	-1.20	110	-1.70	83	-2.51
3	-0.64	-1.21	110	-1.71	87	-2.51

[a] Measured at 0.1 V×s^{-1}. [b] Peak potential value for irreversible processes.

The CV of the ligand phterpy (Figure S14) showed only one reversible reduction at -2.36 V in the potential range –2.5 ÷ +1.2 V (*vs* FeCp$_2$), according to literature.[32] When phterpy was coordinated to the Pt(II) centre in **1**, three reduction processes appeared in the solvent potential window, red trace in Figure

3. The analysis of the cyclic voltammetric response at different scan rates (between 0.02 and 1.00 V×s^{-1}) confirmed that the redox change at -1.21 V is electrochemically quasi reversible, while the one at -1.70 V is electrochemically and chemically reversible, diffusion-controlled, one-electron process;[33] the reduction occurring at the more negative potential (-2.51V) is irreversible. Considering slightly different compounds, Hill *et al.*[34] indicated that the first reduction was essentially ligand based, the second could have a partial metal character and the third could be associated to the loss of Cl$^-$ from the complex. On the other hand, it was proposed by Ziessel *et al.*[35] that the second reduction could be again based on terpyridine. Also, in our experimental conditions, we found no indications of chloride dissociation after the third reduction, because we did not see the wave associated to the oxidation process Cl$^-$ → 1/2Cl$_2$ during the following positive scan.

2 and **3** undergo four sequential reductions, Figure 3. The process named E$_a$ is an irreversible reduction which occurs at -0.29 V for **2** and at -0.64 V for **3**. Scanning toward more negative potential, the processes E$_1$, E$_2$ and E$_3$ occur at the same potential of **1**. Hydrodynamic voltammetry (indicated LSV, linear sweep voltammetry) at a glassy-carbon rotating disk electrode showed that the limiting current of E$_a$ for both **2** and **3** was two times that of the reversible reductions (E$_1$ and E$_2$, displayed in Figures S15-S16, SI). Therefore we propose that E$_a$ is a two-electron reduction step centred on the metal, relative to the Pt(IV) → Pt(II) reduction. The Pt(II) just formed rapidly decomposes with release of two ligands, which makes the process irreversible in the potential window examined. The Pt(II) species, formed after E$_a$, arranges in aggregates at the electrode surface and undergoes the reduction processes already described for **1** (see Figure S17 SI).

In order to demonstrate that E$_a$ is the reduction process that produces the Pt(II) species, we performed an electrolysis on a solution of **2**, setting the potential at -0.5 V (E$_a$ was -0.29 V). We could recognize the species produced during the electrolysis with a simple UV-Vis analysis, because the Pt(II) and the Pt(IV) species exhibit very different absorption spectra and it is easy to discriminate between them (Figure S18 SI). Before the electrolysis all the Pt present was in the +4 oxidation state but, after the process, the Pt(II) species **1** was clearly identified from its absorption band at 405 nm. Its concentration could be assessed by interpolation of the height of the peak at 405 nm with a calibration curve (Figures S19-S20 SI), giving an amount of Pt(II) that was the 37% of the initial Pt(IV). We could also calculate the percentage of reduction taking into account the quantity of charge that passed through the electrodes, which was measured by the software during the electrolytic process (as explained in the experimental section). This percentage, for a bi-electronic process, roughly corresponds to the 37% of the initial platinum present, in good agreement with the value obtained with UV-Vis spectroscopy.

In the case of **3** we verified that the peak E_a (-0.64 V) is attributable to the reduction Pt(IV) → Pt(II) by firstly irradiating a solution of **3** with the UV lamp and then studying the outcome with electrochemical methods, see section S4 and Figure S21 in SI.

The major observable difference between **2** and **3** is the 350 mV more favourable reduction potential for the former. According to the donor strength of the two axial ligands, chlorides for **2** and acetates for **3**, the easier reduction of **2** is justifiable.[36] Indeed, Ellis *et al.*[7] reported that the cathodic reduction potential of a Pt(IV) is mainly dependent on the electron withdrawing power of the axial ligands. Like us, they found a difference between the reduction potential of a Pt(IV) with axial acetates and with axial chlorides of 320 mV, in aqueous solvent. In our case the poor solubility of **2** and **3** in water prevented an electrochemical investigation in aqueous solution, however we tested the two compounds in a mixture 1:1 DMSO:phosphate buffer solution (PBS, Na_2HPO_4/KH_2PO_4, $\Sigma c_{(PO4)}$ = 0.01 M, pH = 7.4, NaCl 0.137 M). The voltammetric profile in both cases exhibits an irreversible and broad reduction peak at +0.17 V for **2** and at -0.33 V for **3** (data not shown). By comparison with the CV in DMSO, we assigned this redox process to the metal-centred Pt(IV) → Pt(II) reduction, therefore we can presume that also in neat aqueous solution (and in the cellular environment) the complex with axial chlorides is more easily reducible than the one with axial acetates.

Cell studies

The reduction potential evaluated with electrochemistry can have a profound effect on the activity of the compounds in killing the cells. It is known that the ease of reduction of a Pt(IV) compound in a biological medium is an essential parameter to consider, since the anticancer activity is exerted only after the reduction to the Pt(II) species.[37] Therefore, in the cytotoxicity studies of this paragraph, we expect that a high toxicity reflects a low stability, and viceversa. The data for the cell viability of two ovarian carcinoma A2780 and A2780cis cell lines (sensitive and resistant to cisplatin, respectively) are summarized in Table 2 and in the sigmoidal curves of Figure S22 (SI). Cisplatin was used as reference.

Table 2. Viability studies for A2780 and A2780cis ovarian cell lines. The IC_{50} values, obtained after a 72 hours treatment in the dark, are reported in μM with their standard deviation.

Compound	IC_{50}	
	A2780	A2780cis
cisplatin	0.40 ± 0.07	7.2 ± 0.6

Compound	IC$_{50}$	
	A2780	A2780cis
phterpy	0.61 ± 0.06	1.7 ± 0.2
1	11.5 ± 0.7	9.4 ± 0.9
2	9.4 ± 0.9	10.5 ± 0.8
3	16 ± 1	30 ± 1

The ligand phterpy displays high toxicity against both the sensitive and the resistant cell lines, probably because of the complexation to metal ions in the biological medium, as already found for similar species.[39] The fact that the IC$_{50}$ of **1** is considerably higher than that of phterpy indicates that the ligand does not dissociate from the platinum metal center when the complex is in contact with biological targets. **1** and **2** have similar IC$_{50}$ values in both cell lines, considering the statistical errors. This behavior could be explained considering that **2** has a low reduction potential, so it could be reduced to Pt(II) once inside the cells, making the IC$_{50}$ of **1** and **2** similar. On the other hand, **3** is less easily reducible and, therefore, its IC$_{50}$ values are higher. To prove this point we studied the interaction of the complexes with one of the most abundant and effective reducing agent in the cell, the tripeptide glutathione (GSH) [riferimento che dice che il GSH è proprio uno dei più forti e abbondanti riducenti cellulari, Chiara], Figures S23-S25 SI. The UV-Vis spectra suggested that **1** readily substituted its chloride ligand for the thiol ligand (Figure S23 SI) and that **2** was reduced instantaneously to a Pt(II) species, which in turn coordinated the thiol group (Figure S24 SI). On the other hand, **3** did not interact rapidly with GSH, but only after a few hours there was an appreciable change in the absorption spectrum. The reaction was found to be not complete after 24 hours (Figure S25 SI).

Phototoxicity

Considering that **3** is more rapidly photoreduced to the Pt(II) active species in physiological-like conditions (Table S1 SI) and that it is more stable in the reducing cellular environment (Figure S25 SI) with respect to **2**, we tested it as a prodrug activated with light. Similarly to Mackay et al.[23] we incubated **3** and cisplatin for 1 hour with A2780 and A2780cis cell lines and then we irradiated the culture plate for 6 minutes at 365 nm, for a total light dose of 2 J×cm^{-2} (5 J×cm^{-2} in Ref. 23). Right after the irradiation the cells were thoroughly washed to remove any trace of non internalized compound, incubated in complete growth medium for 24 hours (recovery time) and then submitted to viability assay. The results of the experiments performed with and without irradiation indicated that **3** was light activated: the viability of

A2780 and A2780cis cell lines was lowered in a dose dependent manner, as reported in Table 3 (IC_{50}) and in Figure S26 (SI, sigmoidal curves).

Table 3. IC_{50} values of **3** and cisplatin, obtained in the phototoxicity study against A2780 and A2780cis ovarian cell lines. The values in the dark and under irradiation are compared.

| Compound | IC_{50} | | Conditions |
	A2780	A2780cis	
cisplatin	379 ± 9	> 500	Dark
3	~ 50	> 50	
cisplatin	314 ± 4	471 ± 6	Light
3	15 ± 1	22 ± 1	

Also cisplatin resulted to be slightly more active when irradiated, probably because UV light induces a faster release of the chloride ligand and formation of active aqua species [Perumareddi, J. R.; Adamson, A. W. Photochemistry of complex ions. V. The photochemistry of some square-planar platinum(II) complexes. J. Phys. Chem. 1968, 72, 414-420.], but this increase is much lower for cisplatin with respect to **3**. Indeed, in the case of the A2780 cell line, the IC_{50} of cisplatin after irradiation is the 80% of its value in the dark, while the IC_{50} of **3** after irradiation is the 30% of its value in the dark.

In addition, since UV light is known to damage healthy cells, we had to verify that the viability of the control cells was unaffected after irradiation. Figure S27 (SI) confirms this point, showing that the viability of the control cells kept in the dark was not statistically different from the one of the control cells exposed to UV light.

Finally, in order to explain such a difference in IC_{50} between cisplatin and **3**, an uptake experiment was carried out. We expected a higher degree of internalization for **3**, because its lipophilicity is higher, as the *logP* evaluation indicated (Table S1, SI). But surprisingly, ICP-AES determination revealed that the cell internalization was the same for **3** and for cisplain (Table S3, SI). So the difference in IC_{50} should be related to a different intrinsic activity. We could speculate that the higher activity of **3** may rely on its higher inertness, preserving the complex from unwanted in-cell-reactions that cisplatin undergoes and that cause its partial inactivation. In any case, the difference in activity opens up a plethora of possible interpretations and only further biological studies could shed light on the actual mechanism of action.

Interaction with small biomolecules

After the investigation of the phototoxic behaviour of compound **3**, we wanted to know how it interacted with biological targets. These studies, conducted in the presence and in the absence of irradiation, could give us further information on how the toxicity is exerted. Therefore, we firstly selected a simplified oligonucleotidic model containing the GG motif (that represent the preferential binding site for Pt-containing molecules) to study the binding toward DNA. We employed the oligonucleotide ODN2, which has the sequence CTACGGTTTCAC, with a molecular weight of 3596.36 Da. Compound **1**, which is most likely the product of the photoreduction, was incubated with ODN2 and originated a peak at 4097.70 Da, due to the formation of the adduct between the biomolecule and the ion fragment $[Pt(phterpy)]^{2+}$, Figure 4A and Figure S28 (SI). We did not observe under any circumstance the binding of the naked Pt(II) cation, proving the fact that the tridentate ligand remains tightly bound, as it was anticipated in the cell studies (*vide infra*).
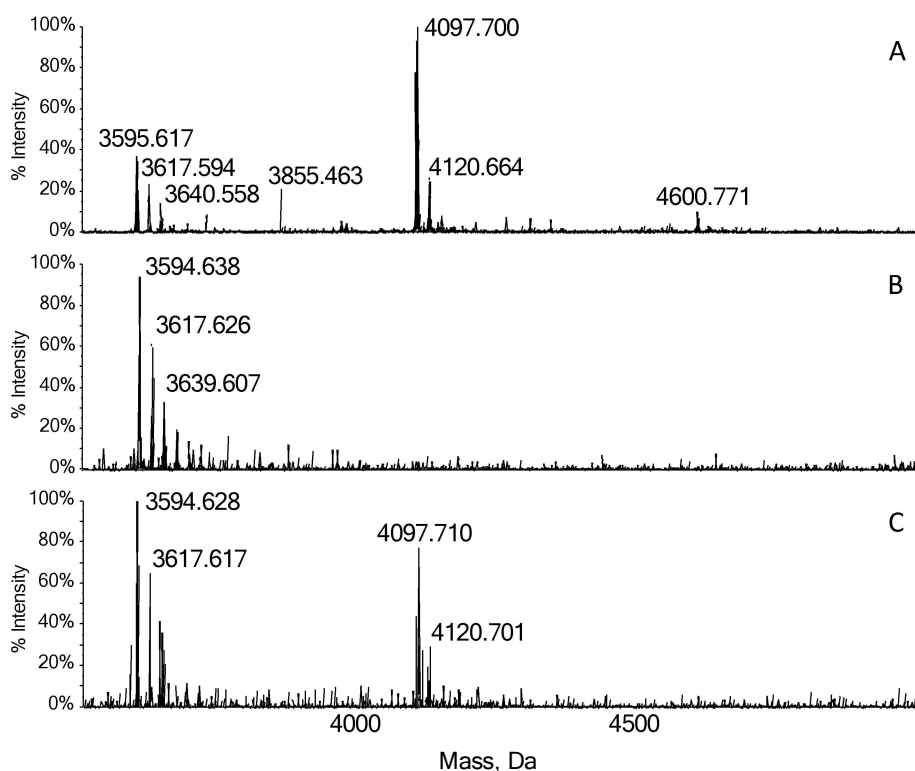

Figure 4. Deconvoluted ESI mass spectrum of **1** incubated for 72 h with ODN2 10^{-4} M (1:1 metal to oligonucleotide molar ratio) at 25 °C in MilliQ water (Panel A); deconvoluted ESI mass spectrum for **3** incubated for 72 h in the dark with ODN2 10^{-4} M (1:1 metal to oligonucleotide molar ratio) at 25 °C in MilliQ water (Panel B); deconvoluted ESI mass spectrum for **3** irradiated for 5 minutes at 365 nm and

incubated for 72 h with ODN2 10^{-4} M (1:1 metal to oligonucleotide molar ratio) at 25 °C in MilliQ water (Panel C).

When **3** was incubated in the dark with the biomolecule, Figure 4B, there was no visible interaction between them in the diagnostic window. The only peak present in the spectrum was the one of the biomolecule (Figure S29 SI), so the stability and inertness of **3** was again confirmed with ESI mass studies. On the contrary, when UV light was used, the reactivity pattern of compound **3** was completely different toward ODN2, showing an extensive interaction with the biomolecule, Figure 4C. The peak at 4097.71 Da was ascribed to the ODN2/[Pt(phterpy)]$^{2+}$ species, pointing out an important reactivity, consequence of the photoreduction of **3**. Compound **2** behaves similarly to **3**, even though some binding to the biomolecule was visible in the ESI mass spectrum of the system kept in the dark (Figures S31÷S32 SI), because of its minor stability.

The second biological target we employed was the small model protein Ribonuclease A, selected to gain a broader view on the reactivity behavior of these photoactivated compounds. The RNase A (type XII-A) used in the studies has a molecular weight of 13681 Da. **1** forms adducts with the protein in a similar way with respect to the oligonucleotide, with dissociation of the chloride ligand and retention of the tridentate nitrogen ligand. The ion fragment [Pt(phterpy)]$^{2+}$ probably binds at a histidine binding site,[38] originating the signal at 14183.3 Da (Figure S33 SI). **2** and **3** kept in the dark showed that the interaction with RNAse A was absent but, when irradiated (365 nm) for 5 minutes, the signal of the adduct was again detectable, similarly to **1** (Figures S34÷S37). The data obtained with the RNAse A corroborate our deduction that the Pt(IV) has to be reduced to a Pt(II) species with light, before being able to dissociate the chloride ligand and to bind to the biomolecule.

Interaction with CT-DNA

Our last goal was to study how compound **1** and CT-DNA (helix B, in this paragraph named **P**) interacted with one another, to see if there was intercalation or direct binding. To discriminate between the two possible ways of interaction, we performed some spectrophotometric titrations at different temperatures, to obtain the values of the thermodynamic functions H and S.

1 in aqueous sodium cacodylate was titrated with **P** and an absorption spectrum was recorded after each addition (Figure 5). The change in the shape of the absorption spectrum is significant of the interaction between **1** and **P**. This interaction was evaluated by reporting the variation of the signal intensity (ΔA, normalized against the concentration of **1**) as a function of the concentration of **P** at λ = 370 nm. The quantitative analysis of the binding should be done preferably at wavelengths higher than 300 nm, to avoid free DNA excess interference with the diagnostic signal. The resulting binding isotherm (Figure 5,

inset) reveals two different steps for the interaction. At low **P** concentration (first branch) the excess of **1** can lead to cooperative aggregation on the helix and relevant complicate stoichiometries. However, under **P** excess conditions (second branch), the system is likely to be devoid of cooperative processes.
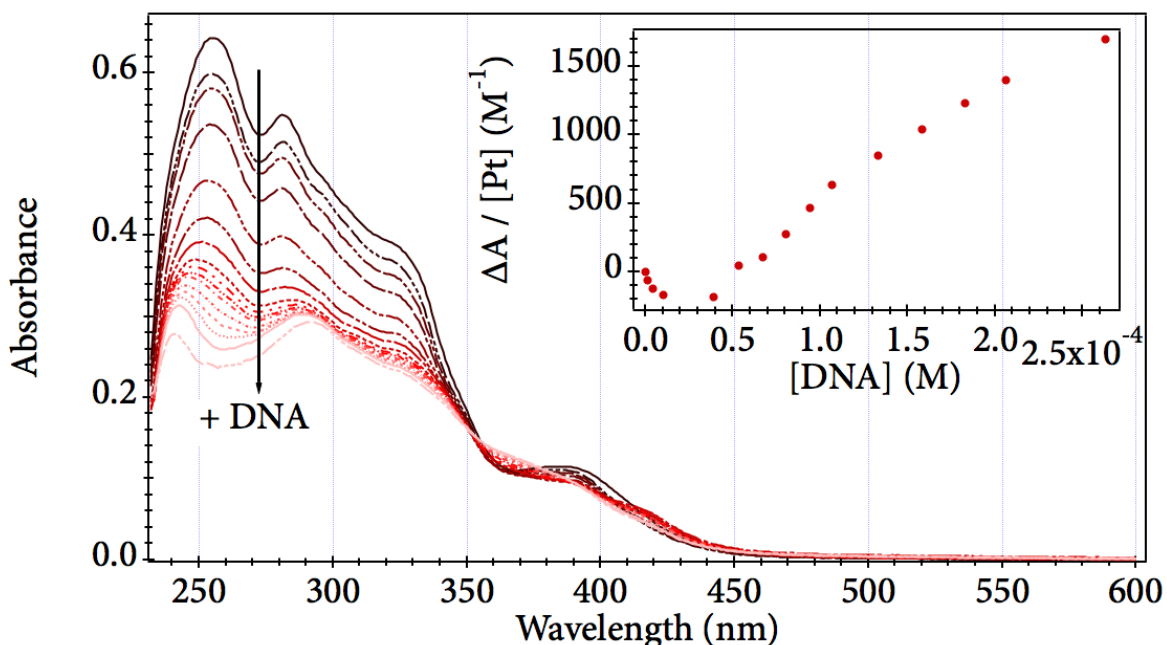

Figure 5. Spectrophotometric titration of **1** (2×10^{-5} M) with increasing amounts of DNA; insight: binding isotherm at 370 nm. DNA concentration goes from 0 to 2.6×10^{-4} M, [NaCac] = 0.1 M, pH = 7.3, [Cl]$^-$ = 7×10^{-3} M, DMSO content was less than 2%, T = 25.0 °C.

Equilibrium constants were obtained with the software Hypspec2014[®] under these latter conditions at different temperatures: at 18.6 °C $K_{eq} = 9.3 \times 10^4$, at 25.0 °C $K_{eq} = 1.7 \times 10^5$ and at 36.5 °C $K_{eq} = 2.5 \times 10^5$. The fitting procedure (shown in Figure S38 SI) uses the **1$_2$P** species as a way to weight the cooperative effects but confirmed the majority formation of the monoadduct (**1P**). From the linear plot of $\ln K_{eq}$(**1P**) against the reciprocal temperature (Figure S39 SI, Van't Hoff equation) we get $\Delta H = 9.3$ kcal×mol^{-1}, ΔS = 0.055 kcal×mol^{-1} and $T\Delta S = 16$ kcal×mol^{-1} at 298K. Being ΔH strongly positive we can conclude that Entropy directs the spontaneity of the reaction and that the prevailing binding mode is non-intercalative and directed to the helix grooves.[30] Also, ΔH is quite high compared to other species, which means that the covalent binding to a nitrogen base should be a non-negligible event, as it was reported also by other authors.[31]

Some absorption tests confirmed that compound **3** does not interact with CT-DNA in the dark (Figure S40 SI), again confirming that the Pt(IV) complex is stable and that the reduction to the more reactive

Pt(II) species is needed for the biological activity, as already reported in literature[37] and in the ESI-MS studies for our compounds (*vide infra*).

Conclusions

Pt(IV) prodrugs, to be used in photo-chemotherapy, have to be stable toward reduction and inert toward substitution when kept in the dark in the cellular environment. Also, they have to rapidly transform to active Pt(II) species after irradiation in the visible range of wavelengths. Our preliminary results indicate that complex **3**, [Pt(OCOCH$_3$)$_2$Cl(phterpy)][CF$_3$SO$_3$], partially matches these criteria showing a potentiated activity against A2780 and A2780cis cell lines when photo-activated with a small dose of 365 nm light.

Overall, **3** was found to be a better candidate than **2** for several reasons. It has a more negative reduction potential and shows a very slow reduction in the presence of millimolar amounts of glutathione, confirming the stabilization effect of axial acetates with respect to chlorides. The rate of reduction in aqueous solvent was faster and, finally, its cytotoxicity in the dark was lower. In a comparative study with cisplatin, **3** showed a markedly higher cytotoxicity as a consequence of irradiation after a small period of incubation, even if the cell internalization was found to be the same for the two compounds.

The interactions between **3** and model biological targets pointed out that the binding happened only as a consequence of irradiation. Once reduced, the Pt(II) species dissociated the chloride ligand and the fragment [Pt(phterpy)]$^{2+}$ could bind to the biomolecules. Moreover, the study involving DNA and the Pt(II) species [PtCl(phterpy)][CF$_3$SO$_3$], which is possibly the product of photoreduction of **2** and **3**, suggested that intercalation is not the predominant mode whereas the possible major driving force for interaction is the covalent binding.

SUPPORTING INFORMATION

Selected ^{1}H and ^{195}Pt NMR spectra, UV-Vis spectra, Electrochemical experiments (CV and LSV), ESI mass spectra, 72-hours viability tests (PDF).

REFERENCES

(1)   Giandomenico, C. M.; Abrams, M. J.; Murrer, B. A.; Vollano, J. F.; Rheinheimer, M. I.; Wyer, S. B.; Bossard, G. E.; Higgins, J. D. III. Carboxylation of Kinetically Inert Pt(IV) Hydroxy Complexes. En Entrée into Orally Active Pt(IV) Antitumor Agents. *Inorg. Chem.* **1995**, *34*, 1015-1021.

(2)   Park, G. Y.; Wilson, J. J.; Song, Y.; Lippard, S. J. Phenanthriplatin, a monofunctional DNA-binding platinum anticancer drug candidate with unusual potency and cellular activity profile. *Proc. Natl. Acad. Sci. U. S. A.* **2012**, *109*, 11987-11992.

(3) Sava, G.; Alessio, E.; Bergamo, A.; Mestroni, G. In *Topics in Biological Inorganic Chemistry*; Clarke, M. J., Sadler, P. J. Eds.; Springer: Berlin, 1999; Volume 1, "Metallo Pharmaceuticals", pp 143-169.

(4) Meier-Menches, S. M.; Gerner, C.; Berger, W.; Hartinger, C. G.; Keppler, B. K. Structure–activity relationships for ruthenium and osmium anticancer agents – towards clinical development. *Chem. Soc. Rev.* **2018**, *47*, 909-928.

(5) Johnstone, T.; Suntharalingam, K.; Lippard, S. J. The Next Generation of Platinum Drugs: Targeted Pt(II) Agents, Nanoparticle Delivery, and Pt(IV) Prodrugs. *Chem. Rev*. **2016**, *116*, 3436-3486.

(6) van der Veer, J. L.; Peters, A. R.; Reedijk, J. Reaction Products from Platinum(IV) Amine Compounds and 5'-GMP Are Mainly bis(5 '-GMP)Platinum(II) Amine Adducts. *J. Inorg. Biochem.* **1986**, *26*, 137-142.

(7) Ellis, L. T.; Er, H. M.; Hambley, T. W. The Influence of the Axial Ligands of a Series of Platinum(IV) Anti-Cancer Complexes on their Reduction to Platinum(II) and Reaction with DNA. *Aust. J. Chem.* **1995**, *48*, 793-806.

(8) Balzani, V.; Carassiti, V. *Photochemistry of coordination compounds,* Academic Press: London, 1970.

(9) Kratochwil, N. A.; Bednarski, P. J.; Mrozek, H.; Vogler, A.; Nagle, J. K. Photolysis of an iodoplatinum(IV) diamine complex to cytotoxic species by visible light. *Anti-Cancer Drug Des.* **1996**, *11*, 155-171.

(10) Rosenberg, B.; Van Camp, L.; Trosko, J. E.; Mansour, V. H. Platinum compounds: a new class of potent antitumor agents *Nature*, **1969**, *222*, 385-386.

(11) (a) Müller, P. Schröder, B.; Parkinson, J. A.; Kratochwil, N. A.; Coxall, R. A.; Parkin, A.; Parsons, S.; Sadler, P. J. Nucleotide Cross-Linking Induced by Photoreactions of Platinum(IV)-Azide Complexes. *Ang. Chem. Int. Ed.* **2003**, *42*, 335-339. (b) Mackay, F. S.; Woods, J. A.; Moseley, H.; Ferguson, J.; Dawson, A.; Parsons, S.; Sadler, P. J. A Photoactivated trans-Diammine Platinum Complex as Cytotoxic as Cisplatin. *Chem. Eur. J.* **2006**, *12*, 3155-3161. (c) Farrer, N. J.; Woods, J. A.; Salassa, L.; Zhao, Y.; Robinson, K. S.; Clarkson, G.; Mackay, F. S.; Sadler, P. J. A potent *trans*-diimine platinum anticancer complex photoactivated by visible light. *Ang. Chem. Int. Ed.*, **2010**, *49*, 8905-8908.

(12) Gabano, E.; Perin, E.; Fielden, C.; Platts, J. A.; Gallina, A.; Rangone, B.; Ravera, M. How to obtain Pt(IV) complexes suitable for the conjugation to nanovectors from the oxidation of [PtCl(terpyridine)]$^+$. *Dalton Trans.* **2017**, 10246-10254.

(13) Wang, J.; Hanan, G. S. A Facile Route to Sterically Hindered and Non-Hindered 4'-Aryl-2,2':6',2''-Terpyridines. *Synlett.* **2005**, *8*, 1251-1254.

(14) Nichol, J. C.; Sandin, R. B. The Identification of Aryl Iodides. *J. Am. Chem. Soc.* **1945**, *67*, 1307-1308.

(15) McDermott, J. X.; White, J. F.; Whitesides, G. M. Thermal Decomposition of Bis(phosphine)platinum(II) Metallocycles. *J. Am. Chem. Soc.* **1976**, *98*, 6521-6528.
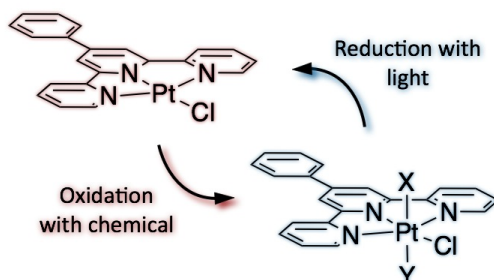
(16) Büchner, R.; Cunningham, C. T.; Field, J. S.; Haines, R. J.; McMillin, D. R.; Summerton, G. C. Luminescence properties of salts of the [Pt(4'Ph-terpy)Cl]$^+$ chromophore: crystal structure of the red form of [Pt(4'Ph- terpy)Cl]BF$_4$ (4'Ph-terpy = 4'-phenyl-2,2':6',2''-terpyridine). *Dalton Trans.* **1999**, 711-717.

(17) a) Baker, M. V.; Barnard, P. J.; Berners-Price, S. J.; Brayshaw, S. K.; Hickey, J. L.; Skelton, B. W.; and White, A. H. Cationic, linear Au(I) N-heterocyclic carbene complexes: synthesis, structure and anti-mitochondrial activity. *Dalton trans.*, **2006**, 3708-3715; b) Marzo, T.; Pillozzi, S.; Hrabina, O.; Kašpárková, J.; Brabec, V.; Arcangeli, A.; Bartoli, G.; Severi, M.; Lunghi, A.; Totti, F.; Gabbiani, C.; Quiroga, A. G.; Messori, L. *cis*-PtI$_2$(NH$_3$)$_2$: a reappraisal. *Dalton Trans*. **2015**, *44*, 14896-14905.

(18) Busto, N.; Valladolid, J.; Aliende, C.; Jalon, F.; Manzano, B. R.; Rodriguez, A. M.; Gaspar, J. F.; Martins, C.; Biver, T.; Espino, G.; Leal, J. M.; Garcia, B. Preparation of Organometallic Ruthenium-Arene-Diaminotriazine Complexes as Binding Agents to DNA. *Chem Asian J.* **2012**, *7*, 788-801.

(19) Felsenfeld, G.; Hirschman, S. Z. A neighbor-interaction analysis of the hypochromism and spectra of DNA. *J. Mol. Biol.* **1965**, *13*, 407-427.

(20) Gagné, R. R.; Koval, C. A.; Lisensky, G. C. Ferrocene as an internal standard for electrochemical measurements. *Inorg. Chem*. **1980**, *19*, 2854-2855.

(21) (a) Michelucci, E.; Pieraccini, G.; Moneti, G.; Gabbiani, C.; Pratesi, A.; Messori, L. Mass spectrometry and metallomics: a general protocol to assess stability of metallodrug-protein adducts in bottom-up MS experiments. *Talanta* **2017**, *167*, 30-38; (b) Biancalana, L.; Pratesi, A.; Chiellini, F.; Zacchini, S.; Funaioli, T.; Gabbiani, C.; Marchetti, F. Ruthenium arene complexes with triphenylphosphane ligands: cytotoxicity towards pancreatic cancer cells, interaction with model proteins, and effect of ethacrynic acid substitution. *New J. Chem*. **2017**, *41*, 14574-14588; (c) Marzo, T.; Cirri, D.; Gabbiani, C.; Gamberi, T.; Magherini, F.; Pratesi, A.; Guerri, A.; Biver, T.; Binacchi, F.; Stefanini, M.; Arcangeli, A.; Messori, L. Auranofin, Et$_3$PAuCl, and Et$_3$PAuI Are Highly Cytotoxic on Colorectal Cancer Cells: A Chemical and Biological Study. *Med. Chem. Lett.* **2017**, *8*, 997-1001.

(22) Solár, P.; Horváth, V.; Kleban, J.; Koval', J.; Solárová, Z.; Kozubík, A.; Fedoročko, P. Hsp90 inhibitor Geldanamycin increases the sensitivity of resistant ovarian adenocarcinoma cell line A2780cis to cisplatin. *Neoplasma* **2007**, *54*, 127-130.

(23) Mackay, F. S.; Woods, J. A.; Heringová, P.; Kašpárková, J.; Pizarro, A. M.; Moggach, S. A.; Parsons, S.; Brabec, V.; Sadler, P. J. A potent cytotoxic photoactivated platinum complex. *Proc. Nat. Acad. Sciences* **2007**, *104*, 20743-20748.

(24) Dunham, S. O.; Larsen, R. D.; Abbott, E. H. Nuclear magnetic resonance investigation of the hydrogen peroxide oxidation of platinum(II) complexes. Crystal and molecular structures of sodium trans-dihydroxobis(malonato)platinate(IV) hexahydrate and sodium trans-dihydroxobis(oxalato)platinate(IV) hexahydrate. *Inorg. Chem.* **1993**, *32*, 2049-2055.

(25) Macias, F. J.; Deo, K. M.; Pages, B. J.; Wormell, P.; Clegg, J. K.; Zhang, Y.; Li, F.; Zheng, G.; Sakoff, J.; Gilbert, J.; Aldrich-Wright, J. R. Synthesis and Analysis of the Structure, Diffusion and Cytotoxicity of Heterocyclic Platinum(IV) Complexes. *Chem. Eur. J.* **2015**, *21*, 16990-17001.

(26) Arena, G.; Monsù Scolaro, L.; Pasternack, R.; Romeo R. Synthesis, Characterization, and Interaction with DNA of the Novel Metallointercalator Cationic Complex (2,2':6',2''-Terpyridine)methylplatinum(II). *Inorg. Chem.* **1995**, *34*, 2994-3002.

(27) Krause-Heuer, A. M.; Wheate, N. J.; Price, W. S.; Aldrich-Wright, J. R. Diffusion-based studies on the self-stacking and nanorod formation of platinum(II) intercalators. *Chem. Commun.* **2009**, 1210-1212.

(28) Hall, M. D.; Telma, K. A.; Chang, K. E.; Lee, T. D.; Madigan, J. P.; Lloyd, J. R.; Goldlust, I. S.; Hoeschele, J. D.; Gottesman, M. M. Say No to DMSO: Dimethylsulfoxide Inactivates Cisplatin, Carboplatin, and Other Platinum Complexes. *Cancer Res.* **2014**, *74*, 3913-3922.

(29) Ma, E. S. F.; Bates, W. D.; Edmunds, A.; Kelland, L. R.; Fojo, T.; Farrell, N. Enhancement of Aqueous Solubility and Stability Employing a Trans Acetate Axis in Trans Planar Amine Platinum Compounds while Maintaining the Biological Profile. *J. Med. Chem.* **2005**, *48*, 5651-5654.

(30) Chaires, J. B. A thermodynamic signature for drug–DNA binding mode. *Archives Biochem. Biophys.* **2006**, *453*, 26-31.

(31) Safa Shams Abyaneh, F.; Eslami Moghadam, M.; Hossaini Sadr, M.; Divsalar, A. Effect of lipophilicity of amylamine and amylglycine ligands on biological activity of new anticancer cisplatin analog. *J. Biomol. Struct. Dyn.* **2018**, *36*, 893-905.

(32) Constable, E. C.; Lewis, J.; Liptrot, M. J.; Raithby, P. R. The coordination chemistry of 4'-phenyl-2,2':6',2"-terpyridine; the synthesis, crystal and molecular structures of 4'-phenyl-2,2':6',2"-terpyridine and bis(4'-phenyl-2,2':6',2"-terpyridine)nickel(II) decahydrate. *Inorg. Chim. Acta* **1990**, *178*, 47-54.

(33) Zanello, P. *Inorganic electrochemistry: theory, practice and application,* RSC: Cambridge, UK, 2003.

(34) Hill, M. G.; Bailey, J. A.; Miskowski, V. M.; Gray, H. B. Spectroelectrochemistry and Dimerization Equilibria of Chloro(terpyridine)platinum(II). Nature of the Reduced Complexes. *Inorg. Chem.* **1996**, *35*, 4585-4590.

(35) Ziessel, R.; Diring, S.; Retailleau, P. Terpyridine-platinum(II) acetylide complexes bearing pendent coordination units. *Dalton Trans.* **2006**, 3285-3290.

(36) Lever, A. B. P. Electrochemical parametrization of metal complex redox potentials, using the ruthenium(III)/ruthenium(II) couple to generate a ligand electrochemical series. *Inorg. Chem.* **1990**, *29*, 1271-1285.

(37) Hall, M. D.; Hambley, T. W. Platinum(IV) antitumour compounds: their bioinorganic chemistry. *Coord. Chem. Rev.* **2002**, *232*, 49-67 and references therein.

(38) Marzo, T.; Navas, F.; Cirri, D.; Merlino, A.; Ferraro, G.; Messori, L.; Quiroga, A. G. Reactions of a tetranuclear Pt-thiosemicarbazone complex with model proteins. *J. Inorg. Biochem.* **2018**, *181*, 11-17.

(39) McFayden, D. W.; Wakelin, L. P. G.; Roos, I. A. G.; Leopold, V. A. Activity of Platinum(II) intercalating agents against Murine Leukimia L1210. *J. Med. Chem.* **1985**, *28*, 1113.

(40) Johnson, S. W.; Ferry, K. V.; Hamilton, T. C. Recent insights into platinum drug resistance in cancer. *Drug Resistance Updates* **1998**, *1*, 243-254.

(41) Logan, S. R. Does a photochemical reaction have a reaction order? *J. Chem. Educ.* **1997**, *74*, 1303.

FOR TABLE OF CONTENTS ONLY

Two Pt(IV) complexes, synthesized to be used as light-activated compounds, are stable in physiological-like conditions in the dark and undergo photoreduction to the Pt(II) parent compound upon irradiation at 365 nm. One of them showed improved aqueous solubility and a potentiated activity against A2780cis cell lines when photoactivated with light, even with respect to cisplatin. DNA interaction studies suggested DNA as the possible target.